

Article

# Preparation of Fluoroalkyl-Acrylate-Modified Polysiloxane Nanocomposite and Its Surface Properties as a Superhydrophobic Coating Material

Fuquan Deng <sup>1,2</sup>, Hua Jin <sup>3</sup> and Wei Xu <sup>2,4,\*</sup>

<sup>1</sup> College of Art and Design, Shaanxi University of Science and Technology, Xi'an 710021, China; dengfuquan@sust.edu.cn

<sup>2</sup> Zhejiang Wenzhou Research Institute of Light Industry, Wenzhou 325003, China

<sup>3</sup> Wenzhou Vocational and Technical College, Wenzhou 325035, China; jh-skd@163.com

<sup>4</sup> College of Bioresources Chemical and Materials Engineering, Shaanxi University of Science and Technology, Xi'an 710021, China

\* Correspondence: xuwei@sust.edu.cn; Tel.: +86-29-86168235

Received: 3 September 2019; Accepted: 25 September 2019; Published: 27 September 2019



**Abstract:** Based on the as-synthesized modified polysiloxane containing pendant long-chain fluoroalkyl and silanoxyl (PFAS) in our previous work, an in situ condensation reaction with silica sol was carried out to prepare a fluoroacrylate-modified polysiloxane nanocomposite. The polysiloxane nanocomposite was then applied as a fabric finish to construct a superhydrophobic coating. The structural and thermal properties of the polymer, surface morphology, surface composition and hydrophobicity of the fabric coatings, polymer fine microstructure, and performance properties of the treated fabrics were researched using infrared spectrometry, thermogravimetric analysis, scanning electron microscopy, atomic force microscopy, X-ray photoelectron spectrometry, and measurement of the contact angle, whiteness, and softness. The characterization results showed that the product had good thermal stability. The static contact angle and rolling contact angle on the finished fabric surface were 163.5° and 7°, respectively. The whiteness and softness were basically similar to those of untreated fabrics. Moreover, due to the stable covalent bond between the silica particles and the polymers, the static contact angle remained 152.3° after 15 cycles of washing, which indicates that it has good water resistance.

**Keywords:** fluorosilicon copolymer; nanocomposite; superhydrophobic; water resistance; coating

## 1. Introduction

Organosiloxanes have such properties as low glass transition temperature and good film-formation capacity, and they are one of the most characteristic post-softening fabric finishes [1–3]. However, since their surface free energy as a fabric finishing agent is not sufficiently low, the waterproof property of the finished fabric is unsatisfactory. Fluorinated polyacrylate as an oil- and water-repellent finish has a low surface free energy and can supply the finished fabric with the desired hydrophobic and oleophobic effect, but the fabric feels apparently hard after treatment. Meanwhile, the fluorosilicone copolymers have the advantages of both organic fluorine and silicone and have excellent film-forming capacity and extremely low surface energy, and they can provide the required anti-fouling and softness properties of the fabric. Thus, much attention has been given to these polymers in recent years [4–6].

The bionic superhydrophobic fabrics possess water- and oil-proofing, antifouling, and self-cleaning properties and therefore have great market prospects. At present, the preparation methods of the superhydrophobic fabrics mainly include the following: Firstly, the hydrophobic nanoparticles (SiO<sub>2</sub>, TiO<sub>2</sub>, etc.) are prepared by the sol-gel method and are then applied to construct the superhydrophobic

fabrics [7,8], but the nanoparticles easily fall off because of their poor capacity to combine with the fabrics. Secondly, direct assembly of low-surface-energy materials on the surface of the fabric can be used to build superhydrophobic fabrics [9]. Last, but not least, micro-nano coarse structures are produced on the fabric surface by sol-gel, carbon nanotube [10], pulsed laser deposition [11], and vapor deposition [12], and it is then treated with low-surface-energy materials (usually long-chain alkyl, perfluoroalkyl silane, organosilicone, fluorine-containing materials, and resin [13–16]). After this two-step treatment, superhydrophobic fabrics are obtained. However, the above methods or processes are sometimes complicated; the equipment or the silanes are expensive, and defects arise such as slow film formation on the surface of the large void fibers, loose hydrophobic film, and difficulty in coating the film on a large area, which limits their further applications.

Polymer nanocomposites can be used to treat cotton fabrics by simple processes to give them required properties such as wettability, UV proofing, antibacterial properties, and electrical conductivity. Therefore, they have attracted more attention from researchers. To date, they have been prepared by sol-gel, in situ polymerization, and simple physical blending. However, the nanoparticles in the blending tend to agglomerate; the binding force between the nanoparticles and the cotton fabric is also weak; and the powder easily drops off. All these result in poor durability of the relevant fabric properties. By sol-gel and in situ polymerization, the nanoparticles' surface can be chemically modified to promote the combination of the nanoparticles and the polymer matrix so as to overcome the poor durability. Therefore, these two methods are commonly applied to prepare polymer nanocomposites. In addition, polysiloxanes, commonly used in the textile industry, can provide unique properties such as low surface free energy, softness, smoothness, and the feel of silk. As a result, polysiloxane-based nanocomposites can give the fabric good superhydrophobicity, gas permeability, and flexibility after a simple treatment process. In previous work [17,18], we obtained two polysiloxane-based nanocomposite hydrophobic fabric finishes by graft copolymerization and in situ condensation methods, and we then applied them in the one-step treatment of fabric to obtain superhydrophobic fabric with good water resistance. However, a few works have reported the use of fluorosilicone-based nanocomposites as superhydrophobic fabric finishes in recent years.

Building on the above discussion, we aimed to prepare a fluorosilicone-based nanocomposite (PFAS-SiO<sub>2</sub>) by an in situ condensation reaction between silica sol and our pre-synthesized modified polysiloxane containing pendant long-chain fluoroalkyl and silanoxyl (PFAS) [19]. Another purpose was to verify the feasibility of the fabrication of a superhydrophobic fabric coating using this nanocomposite via a simple one-step process. Thus, the structural and thermal properties of the polymer, surface morphology, surface composition and hydrophobicity of the fabric coatings, polymer fine microstructure, and performance properties of the treated fabrics were investigated using infrared spectrometry, thermo gravimetric analysis, scanning electron microscopy, atomic force microscopy, X-ray photoelectron spectrometry, and by measuring the contact angle, whiteness, and softness.

## 2. Materials and Methods

### 2.1. Materials

Fluoroalkyl-acrylate-modified polysiloxane (PFAS) was made in our laboratory, and its viscosity was 860 mPa·s. Nanosilica sol was also prepared in our lab with an average particle size of 134.3 nm and PDI of 0.006, as well as a solid content of 30 wt %. Ethyl acetate of analytically pure grade was supplied by Tianjin Chemical Reagent Co., Ltd., Tianjin, China and purified twice by pre-distillation prior to use. Benzene and isopropanol were both analytically pure and purchased from Sinopharm Chemical Reagent Co., Ltd., Shanghai, China. Silicon wafers were obtained from Shanghai Songjiang Electronic Material Factory, Shanghai, China, and were pretreated and cleaned according to methods in the literature [20–22]. The cloth specimens were pure cotton, and their specifications are shown in Table 1.

Table 1. Cotton fabric specifications.

Fabric Weight (g/m <sup>2</sup> )	Yarn Count		Fabric Density	
	Warp	Weft	End/cm	Picks/cm
119	40	40	133	72

## 2.2. Synthesis of Fluoroalkyl-Acrylate-Modified Polysiloxane Nanocomposites

A quantity of 50 g PFAS and a certain amount of benzene/ethanol mixed solvent and silica sol (20, 40, or 80 g) were added in order into a 250 mL three-neck flask equipped with a stirrer, thermometer, and reflux condensing tube; they were stirred thoroughly and heated to 50 °C, then left to react for 3–4 h. Next, the solvents were removed under reduced pressure to obtain a translucent viscous liquid; this was the fluoroalkyl-acrylate-modified polysiloxane nanocomposite and was denoted PFAS-SiO<sub>2</sub>-1, PFAS-SiO<sub>2</sub>-2, or PFAS-SiO<sub>2</sub>-3. A schematic of the whole synthesis process is shown in Figure 1.

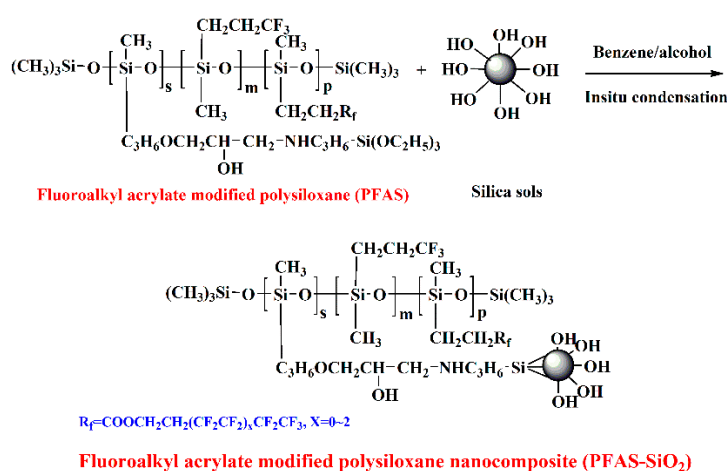


Figure 1. Schematic diagram of the synthesis of PFAS-SiO<sub>2</sub>.

## 2.3. Finishing Process of Cotton Fabric

The pure cotton fabric with the above specifications was clipped into cloth specimens of size 10 × 10 cm<sup>2</sup> which were ultrasonically rinsed using acetone and deionized water, respectively, for 15 min and then dried at 80 °C. Finally, those cloth specimens were put into a desiccator for 24 h to balance.

The PFAS-SiO<sub>2</sub>-3 finishing liquors were respectively prepared using PFAS-SiO<sub>2</sub>-3 and ethyl acetate at mass ratios of 0.1%, 0.2%, 0.3%, 0.4%, and 0.5%. The cotton samples were immersed in the above-mentioned finishing liquids and rolled to control the wet pick-up at 70%. Next, they were dried at 100 °C and then baked at 170 °C for 2 min. Finally, the samples were kept at ambient temperature in a desiccator to balance for 24 h.

## 2.4. Characterization

### 2.4.1. Structural Characterization

#### (1) Infrared Spectroscopy (IR)

The samples were prepared using a KBr coating method and measured on a VECTOR-22 type FT-IR spectrometer (Bruker Company, Billerica, MA, USA).

## (2) XPS Analysis

The chemical composition of the PFAS-SiO<sub>2</sub>-3 film on the fabric surface was analyzed via Axis Ultra type X-ray photoelectron spectroscopy (Kratos Analytical Company, Manchester, UK). The X-ray source was a monochromatic Al K $\alpha$  ray with angular resolution of 90°. The vacuum degree adopted in the analysis chamber was  $1.2 \times 10^{-8}$  Pa. The binding energy deviation caused by the charging effect was corrected by the C 1s peak of carbon pollution (284.8 eV) on the silicon surface.

### 2.4.2. Thermal Stability

The PFAS and a series of PFAS-SiO<sub>2</sub> were allowed to stand at room temperature for 24 h and then tested using a Q500 thermogravimetric analyzer (TA Ltd., New Castle, DE, USA) under a nitrogen atmosphere at a heating rate of 10 °C/min.

### 2.4.3. SEM Observation

The cotton fabrics before and after PFAS-SiO<sub>2</sub>-3 finishing were coated with gold in a vacuum. Then, their surface topographies were observed using an S-4800 scanning electron microscope (Hitachi Ltd., Tokyo, Japan).

### 2.4.4. Fine Film Morphology of PFAS-SiO<sub>2</sub>-3

To obtain the fine film morphology of PFAS-SiO<sub>2</sub>-3 and eliminate the experimental error due to the distortion of soft fabrics or fibers during AFM observation, a silicon wafer was used as the simulated matrix to dip vertically in the PFAS-SiO<sub>2</sub>-3/ ethyl acetate solution (0.3 wt %) for 3–5 seconds. Then, it was taken out and baked at 100 °C for 10 min. Next, it was cured at 160 °C for 1 min and placed in a desiccator to balance at room temperature for 24 h. The sample was observed using a Nanoscope IIIA atomic force microscope (Digital Instrument Co., Tonawanda, NY, USA). The test temperature and the relative air humidity were kept at 22 °C and 39.5%, respectively. AFM images were acquired in tapping mode.

### 2.4.5. Measurement of the Performance Properties of the Fabrics

The hydrophobicities of the cotton fabrics were indicated by the static contact angles on the finished fabric surface. Those were measured using an OCA20 contact angle goniometer (Dataphysics Ltd., Filderstadt, Germany). The volume of water drops adopted was 5  $\mu$ L, and the average of five readings was used as the final value for each sample. The washing durability of the cotton fabric finished with PFAS-SiO<sub>2</sub>-3 was examined by washing the treated fabrics in a washing machine according to the method specified in Australian Standard (AS 2001.1.4).

The whiteness of the fabric was measured using a YQ-Z-48B fluorescent whiteness meter.

The softness of a fabric is normally expressed as the bending rigidity—the smaller the bending rigidity, the better the softness of the fabric. A 10 cm  $\times$  10 cm cloth sample was used, and its bending rigidity was measured using a Drick softness measuring instrument (Drik instrument Co., Ltd., Jinan, China).

## 3. Results and Discussion

### 3.1. Infrared Spectrum Analysis

The structure of PFAS-SiO<sub>2</sub> was confirmed by IR. For comparison, the IR graph of PFAS is also presented. The results are shown in Figure 2.

It can be seen that the absorption peaks of PFAS and PFAS-SiO<sub>2</sub> arose at 2975~2907 and 1452~1377 cm<sup>-1</sup>, 1746, 1213 and 698 cm<sup>-1</sup>, 1274 and 801 cm<sup>-1</sup>, and 1090 cm<sup>-1</sup>, which respectively originate from the stretching vibration absorption peaks and bending vibration absorption peaks of methyl and methylene, the stretching vibration absorption peak of carbonyl, the stretching vibration

absorption peaks and bending vibration absorption peaks of  $-\text{CF}_3$  and  $-\text{CF}_2$  groups, the C–H bending vibration absorption peak and the Si–C stretching vibration absorption peak of Si–CH<sub>3</sub>, and the overlapped stretching vibration absorption peaks of Si–O–Si and C–O–C [20,21]. By comparison with spectrum (a) in Figure 2, we can see that new absorption peaks appeared at 3382 and 468  $\text{cm}^{-1}$  in PFAS-SiO<sub>2</sub>, which should stem from the hydroxyl characteristic absorption peak and bending vibration absorption peak of Si–O–Si in the nanosilica [17,18].

In summary, the as-prepared PFAS-SiO<sub>2</sub> in this study seems to be the expected structure.

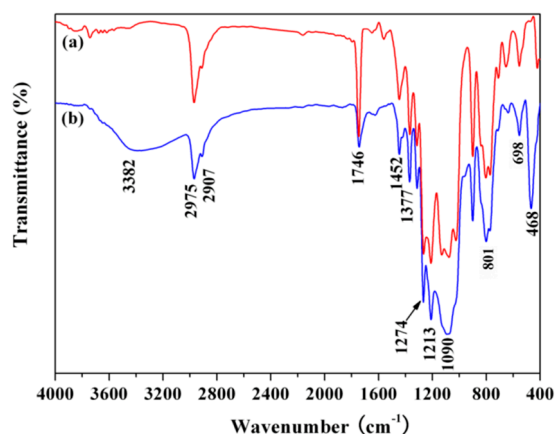


**Figure 2.** The infrared spectrograms of PFAS (a) and PFAS-SiO<sub>2</sub> (b).

### 3.2. Thermal Properties

Figure 3 shows the respective thermogravimetric curves of PFAS, PFAS-SiO<sub>2</sub>-1, PFAS-SiO<sub>2</sub>-2, and PFAS-SiO<sub>2</sub>-3. It can be seen that the initial decomposition temperature of PFAS was 331 °C, and then the weight loss increased rapidly with increasing temperature. When the temperature rose to 570 °C, the mass of polymer PFAS remained unchanged, and the residue was 1.5%. Meanwhile, except for small molecules and some possible solvents in the series of PFAS-SiO<sub>2</sub>, the initial decomposition temperatures and the decomposition temperatures at half weight loss ( $T_{d50}$ ) were both higher than those of PFAS. For example, the  $T_{d50}$  values were 535, 544, 553, and 425 °C for PFAS-SiO<sub>2</sub>-1, PFAS-SiO<sub>2</sub>-2, PFAS-SiO<sub>2</sub>-3, and PFAS, respectively. In addition, the residues of PFAS-SiO<sub>2</sub>-1, PFAS-SiO<sub>2</sub>-2, and PFAS-SiO<sub>2</sub>-3 were, respectively, 7.7%, 17.4% and 25.8%, which indicates that the grafting amounts of the particles in PFAS-SiO<sub>2</sub>-1, PFAS-SiO<sub>2</sub>-2, and PFAS-SiO<sub>2</sub>-3 were probably 6.2%, 15.9% and 24.3% with reference to the result for PFAS (1.5%) and theoretical calculations from the preparation recipes. The above results demonstrate that the introduction of silica particles can increase the thermal stability of PFAS, and the more the combining amount of silica particles, the stronger the thermal stability of PFAS-SiO<sub>2</sub>. The underlying reasons are possibly the high strength and thermal resistance of SiO<sub>2</sub> and their crosslinking effect. Since the silica particles and PFAS polymers were covalently bonded together, thermal motion of the molecule chains would be restricted to some extent, and the thermal stability of the polymer nanocomposites was thus enhanced.

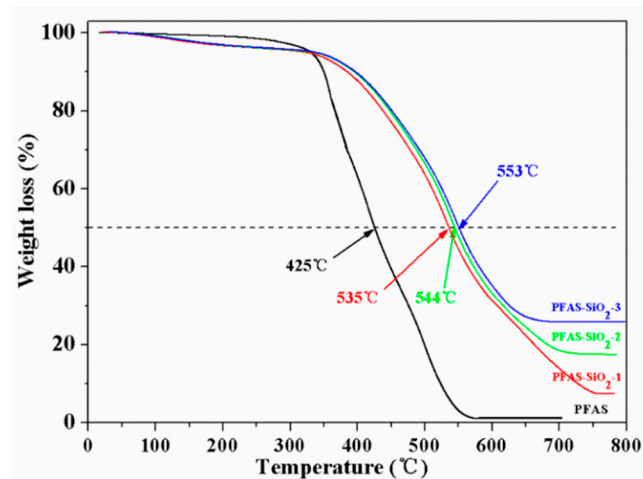


Figure 3. Thermogravimetric diagrams of PFAS and a series of PFAS-SiO<sub>2</sub>.

### 3.3. SEM Observation

In order to theoretically explore the superhydrophobic mechanism of PFAS-SiO<sub>2</sub>-3 coating on the fabric surface, and also to discover the intrinsic relationship between the structure of PFAS-SiO<sub>2</sub> and application performance indicators such as superhydrophobicity and softness, the surface topography of the unfinished fabrics and the PFAS-SiO<sub>2</sub>-3-finished fabrics was observed at different magnifications. The results are shown in Figure 4.

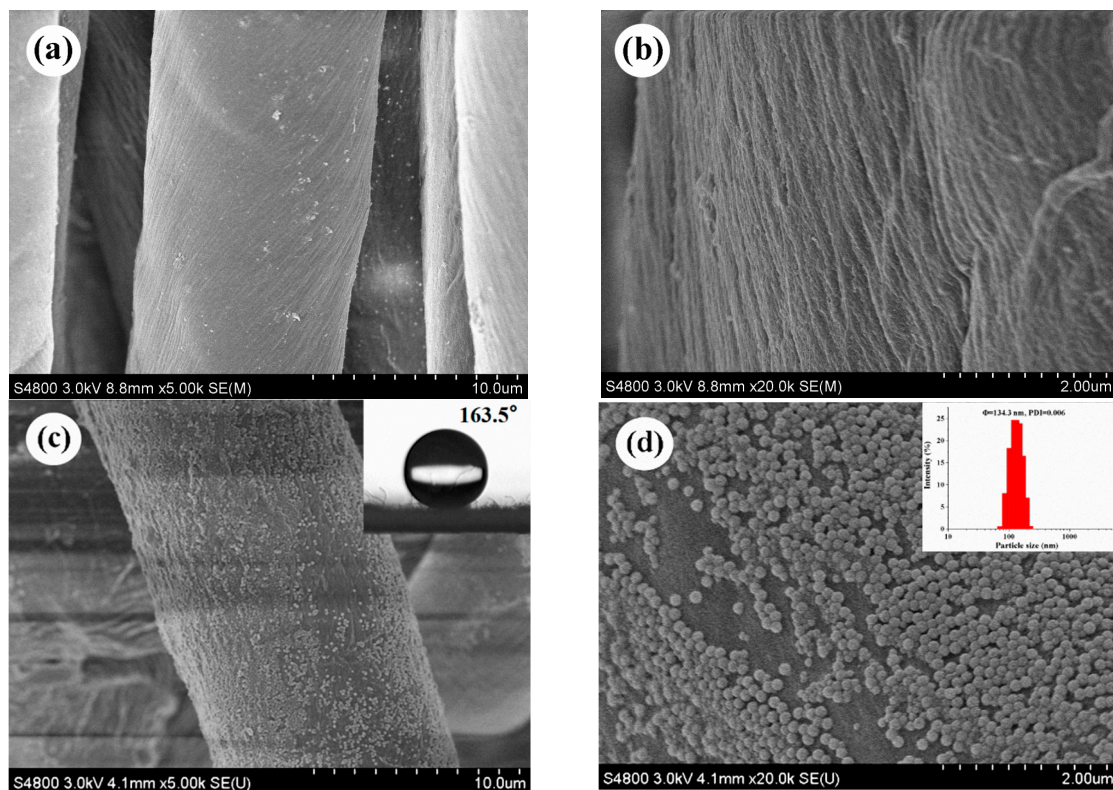


Figure 4. SEM images of unfinished fabric at (a)  $\times 5000$  and (b)  $\times 20,000$  and of PFAS-SiO<sub>2</sub>-3-finished fabric at (c)  $\times 5000$  and (d)  $\times 20,000$ .

It can be seen from Figure 4 that the unfinished blank fiber surface was slightly uneven and rough, and there were many gullies and slurry particles on the surface. However, the PFAS-SiO<sub>2</sub>-3-finished

fiber surface clearly displayed the presence of a large number of particles, which should come from the implanted silica particles and were estimated to be about 100–200 nm in diameter from the scale bar. Apparently, these results are consistent with the mean particle size of the silica sol, as shown in Figure 4d. Besides this, the gullies on the fiber surface basically disappeared, which is due to the covering of the PFAS-SiO<sub>2</sub>-3 hybrid coating on the fiber surface.

### 3.4. AFM Observation

From the above result, we can see that the more precise structure of the PFAS-SiO<sub>2</sub>-3 coating cannot be acquired from SEM observation. Therefore, a higher-resolution instrument was required. The AFM is a new instrument for measuring the fine morphology of polymer films at nanoscale and is often encountered in recent publications [18–21]. So, in this study we also used silicon wafer as the simulated fiber matrix to study the fine morphology of the PFAS-SiO<sub>2</sub>-3 film by AFM, and the results are shown in Figure 5.

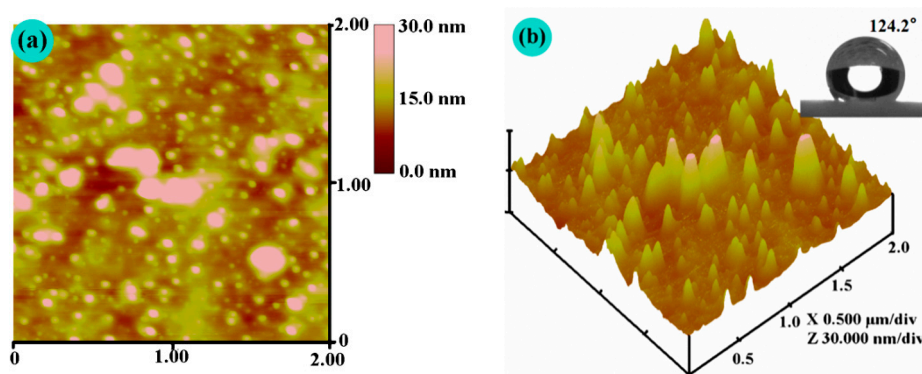


**Figure 5.** AFM diagram of PFAS-SiO<sub>2</sub>-3: (a) height image; (b) three-dimensional image.

It was discovered that a film of PFAS-SiO<sub>2</sub>-3 with inhomogeneous structure was coated on the silicon surface. There were many large peaks and small pinnacles in its 3D topography (Figure 5b), which should be the result of silica particles and interaction with long-chain fluoroalkyl groups. Then, the long-chain fluoroalkyl groups would be curled and intertwined with one another to form small pinnacles extending into the air. Consequently, this arrangement is more conducive to reducing the surface energy of the fiber surface. Moreover, in the scanning range of  $2 \times 2 \mu\text{m}^2$  and at the observing data scale of 30 nm, the root-mean-square roughness of the PFAS-SiO<sub>2</sub> coating was 5.293 nm.

### 3.5. Surface Analysis

To obtain the arrangement information of the various groups in PFAS-SiO<sub>2</sub>-3 on the fabric surface, the chemical composition of the PFAS-SiO<sub>2</sub>-3-finished fabric surface was analyzed by XPS, and the results are shown in Figure 6. The atomic percentage of each element in the PFAS-SiO<sub>2</sub>-3 coating on the fabric surface was obtained from the XPS test results, while the theoretical atomic content of each element was calculated from the experimental formula. The results are shown in Table 2.

The characteristic peaks of F 1s, O 1s, C 1s, Si 2s, and Si 2p in PFAS-SiO<sub>2</sub>-3 film were apparent from the survey XPS spectrum (Figure 6a). However, no obvious N<sub>1s</sub> peaks appeared as a result of the tiny content of nitrogen element. It can be seen from Figure 6b–d that the C 1s peak at the electron binding energy of 284.8 eV was split into a quintet, which indicates that the C elements in PFAS-SiO<sub>2</sub>-3 are in different functional groups. The peaks at 284.8, 286.5, 288.1, 289.6 and 292.6 eV belonged to the carbon elements in the Si–C, C–H, and C–C groups; the C–OH, C–O–C, and C–N groups; the –O–C=O group; the –CF<sub>2</sub>– group, and the –CF<sub>3</sub> group, respectively. In the Si<sub>2p</sub> high-resolution spectrum, the characteristic peaks from the Si–O–Si backbone and SiO<sub>2</sub> could be distinctly observed at 102.6 eV and 103.9 eV. However, the characteristic N<sub>1s</sub> peak could be observed at 399.2 eV in the N 1s high-resolution spectrum. It can be seen from Table 2 that the experimental atomic percentages of

the F, O, C, Si, and N elements were 15.23%, 25.52%, 21.68%, 33.47%, and 4.1%, respectively, while their corresponding theoretical values were 11.24%, 29.94%, 16.86%, 41.85%, and 0.11%, respectively. The measured values of the F and C elements were higher than the theoretical ones, which further confirms that the fluorine-containing groups have a strong tendency to migrate and enrich on the surface during the film-forming process; this will greatly reduce the surface energy of the fiber surface and change it from a hydrophilic surface to a hydrophobic one.

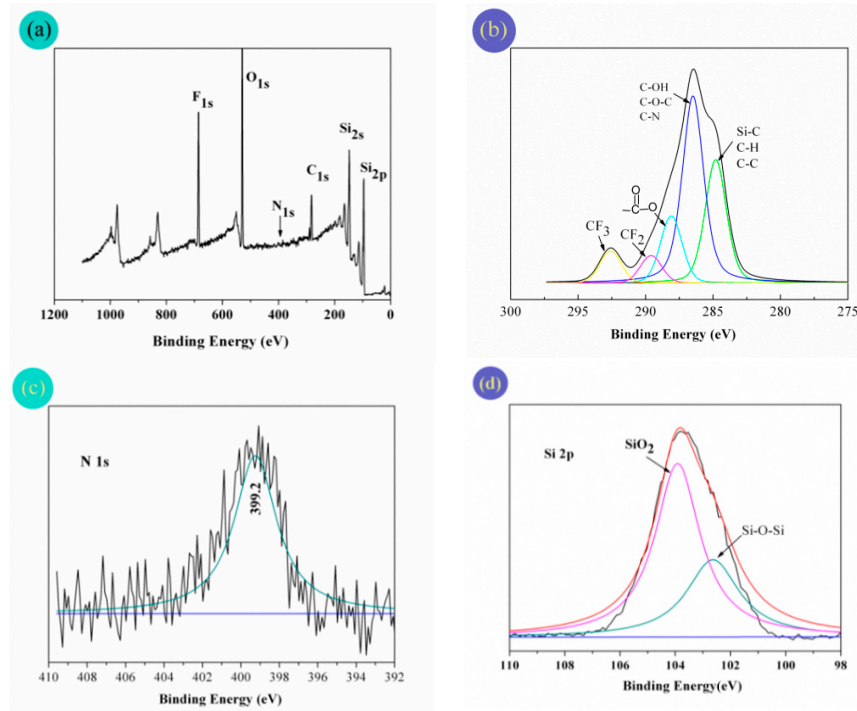


**Figure 6.** XPS survey spectrum (a) and high-resolution C 1s (b), N 1s (c), and Si 2p (d) spectra.

**Table 2.** Atomic composition of the PFAS-SiO<sub>2</sub>-3 film on the fabric surface.

Element	F 1s/% (mass)	O 1s/% (mass)	C 1s/% (mass)	Si 2s/% (mass)	N 1s/% (mass)
Experimental value	15.23	25.52	21.68	33.47	4.10
Theoretical value	11.24	29.94	16.86	41.85	0.11

### 3.6. Performance Properties of the Finished Fabrics

In order to obtain in detail the effects of PFAS-SiO<sub>2</sub>-3 finishing on the fabric's superhydrophobicity, softness, and whiteness, the performance properties of fabrics treated with 0–0.5 wt % PFAS-SiO<sub>2</sub>-3 were measured. The results are shown in Table 3.

**Table 3.** Performance properties of the cotton fabrics treated with PFAS-SiO<sub>2</sub>-3.

Dose of Finishing Agent (g/100 g Ethyl Acetate)	WCA (°)	RCA (°)	Whiteness (°)	BR (mN)	
				w	f
0	0	–	76.89	239	175
0.1	153.6 ± 1.1	15	77.04	235	152
0.2	157.9 ± 1.5	10	77.11	230	149
0.3	161.8 ± 1.3	9	76.98	227	155
0.4	163.4 ± 0.9	7	76.88	237	163
0.5	163.5 ± 1.1	7	76.85	241	170

As can be seen from Table 3, the hydrophobicity of the fabric greatly depended on amount of PFAS-SiO<sub>2</sub>-3 used. The WCA increased greatly and the rolling angle continuously decreased with increasing amount of PFAS-SiO<sub>2</sub>-3. When the PFAS-SiO<sub>2</sub>-3 amount reached 0.4 wt %, the WCA rose to 163.4° and the rolling angle declined to 7°, showing that the treated fabrics achieved the superhydrophobic property. With continued increase in the PFAS-SiO<sub>2</sub>-3 amount, the WCA and the rolling angles remained unchanged, which indicates that the adsorption of PFAS-SiO<sub>2</sub>-3 on the fabric surface becomes gradually saturated when the amount of PFAS-SiO<sub>2</sub>-3 is larger than 0.4 wt %. In addition, with increasing amount of PFAS-SiO<sub>2</sub>-3, the whiteness of the treated fabric was almost the same as that of the blank sample, which indicates that the treatment did not affect the color of the cotton fabric. While the bending rigidity decreased first and then increased, when the PFAS-SiO<sub>2</sub>-3 amount was up to 0.5 wt %, the fabric treated with PFAS-SiO<sub>2</sub>-3 still had better softness than the blank fabric sample. As a fabric finishing agent, PFAS-SiO<sub>2</sub>-3 contains flexible polysiloxane segments and rigid nanoparticles at the same time, but the soft polysiloxane mainchain plays an important role in textile finishing. Thus, with increasing PFAS-SiO<sub>2</sub>-3 amount, at first the softening effect of the flexible polysiloxane chains continually lowers the bending rigidity of the finished fabric. However, when the PFAS-SiO<sub>2</sub>-3 dose was larger than 0.4 g per 100 g ethyl acetate solution, the amount of deposited silica particles on the cotton surface was probably so much that it began to increase the bending rigidity of the finished fabric. Even so, the bending rigidity of the treated fabric was still slightly lower than that of the blank fabric under a PFAS-SiO<sub>2</sub>-3 dose of 0.5 wt %.

### 3.7. Washing Durability of the Treated Fabric

Durability is one of the most important indicators for the practical applications of superhydrophobic cotton fabrics. Therefore, this study evaluated the washing durability of the superhydrophobic fabric according to the standard testing procedure for the washing durability of fabric, and the results are shown in Figure 7. As can be seen from Figure 7, the PFAS-SiO<sub>2</sub>-3-treated cotton fabric still maintained its superhydrophobicity after 15 cycling of washing. After 20 cycles of washing, the WCA was still 147.6°, which shows good water resistance.

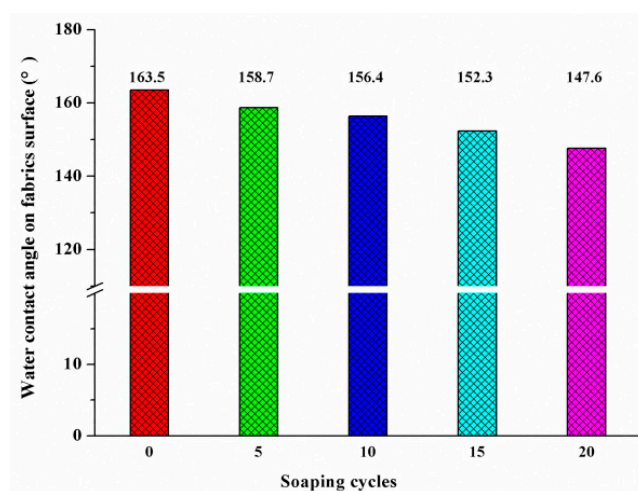


Figure 7. Washing durability of the superhydrophobic fabric.

In the published literature [23,24], to enhance the water resistance of superhydrophobic fabric, the adhesive property of the silica to the fabric is generally improved by crosslinking or by forming covalent bonds between the nanoparticles and the polymers. In the present study, on one hand, covalent bonding was formed in advance by in situ condensation reaction between the pendant reactive silanoxyl and the Si hydroxyl on the silica surface. Then, good interaction between the polymer and the fibers enhanced the binding capacity between particles and fibers. On the other hand, the C–OH in PFAS-SiO<sub>2</sub>-3 generated by the reaction of epoxy groups with amino groups interacted with the

hydroxyls on the fiber surface during the subsequent finishing, coating, and baking process, which enhanced the adhesion of the coating to the fabric fibers. As a whole, good water resistance of the present superhydrophobic fabric was achieved.

### 3.8. Theoretical Model of the Superhydrophobic System

Cotton fabrics are usually textured by fiber bundles and fibrils with different sizes, and they have a coarse and porous surface. Therefore, their theoretical model of superhydrophobicity is explained by the following Cassie equation [25]:  $\cos\theta_c = f_1\cos\theta - f_2$  (1), where  $\theta_c$  is the observed water CA on a rough, porous surface;  $\theta$  is the intrinsic water CA on the corresponding smooth surface;  $f_1$  is the liquid/solid contact area divided by the projected area; and  $f_2$  is the liquid/vapor contact area divided by the projected area. By analyzing the above formulation, it can be understood that the contact angle  $\theta_c$  of the rough solid surface increases when  $f_1$  decreases and  $f_2$  increases. In other words, the greater the proportion of air in the composite surface of the cotton fiber that the water drops touch, the better the hydrophobic properties of the surface.

In the present study, the water contact angle on the PFAS-SiO<sub>2</sub>-3-treated smooth surface, the silicon wafer, was 124.2°, while on the PFAS-SiO<sub>2</sub>-3-treated fabric surface it was 163.5°. According to the Cassie equation, the following results could be obtained:  $f_1 = 0.09$ ,  $f_2 = 0.91$ . That is, when the water drops were in contact with the PFAS-SiO<sub>2</sub>-3 superhydrophobic coating on the cotton surface, only 9% of the area was directly in contact with the cotton fiber substrate, and the rest was in contact with the air. This illustrates that a unique multiscale rough structure with micro/nano/molecular grade was formed among the SiO<sub>2</sub> particles, PFAS with low surface energy, and the coarse cotton fibers, which can contain a large amount of air to form a three-phase composite interface of solid–liquid–gas and which exhibits good superhydrophobic properties and rolling properties.

## 4. Conclusions

A fluoroalkyl-acrylate-modified polysiloxane nanocomposite (PFAS-SiO<sub>2</sub>) was prepared by in situ condensation reaction between a silica sol and a modified polysiloxane (PFAS) containing pendant long-chain fluoroalkyl and silanoxyl. PFAS-SiO<sub>2</sub> was then applied to construct a superhydrophobic fabric coating.

- (1) The synthesized product had the desired structure and good thermal stability.
- (2) The finished fabric had a static contact angle of 163.5° and a lag angle of 7°. The whiteness and softness were basically the same as those before the finish was applied.
- (3) After the superhydrophobic fabric was washed for 15 cycles, the static contact angle on the fabric surface was still 152.3°, showing good water resistance.

**Author Contributions:** Conceptualization, F.D. and W.X.; Methodology, F.D. and W.X.; Formal Analysis, F.D. and W.X.; Investigation, F.D. and W.X.; Data Curation, H.J.; Writing–Original Draft Preparation, F.D.; Writing–Review and Editing, W.X.; Supervision, W.X.; Project Administration, W.X.

**Funding:** This research was funded by the Projects from Key Program of Wenzhou (No. ZG2017028), Basic Scientific Research Program of Wenzhou (No. G20190002), and the Doctorial Research Foundation of Shaanxi University of Science and Technology (No. BJ13-22).

**Conflicts of Interest:** The authors declare no conflict of interest.

## References

1. An, Q.F.; Li, L.S.; Huang, L.X.; Chen, K.C. Film morphology and characterization of functional polysiloxane softeners. *AATCC Rev.* **2006**, *6*, 39–43.
2. Bao, L.H.; Lan, Y.J. Silicone softener for stain repellent stain release and wrinkle resistance fabric finishing. *J. Eng. Fibers Fabr.* **2018**, *13*, 1–5. [[CrossRef](#)]
3. Kang, T.J.; Kim, M.S. Effects of silicone treatments dimensional properties of wool fabric. *Text. Res. J.* **2001**, *71*, 295–300. [[CrossRef](#)]

4. Zhang, G.D.; Hu, Y.Q.; Wu, J.R.; Li, J.Y.; Lai, G.Q.; Zhong, M.Q. Improved synthesis and properties of hydroxyl-terminated liquid fluorosilicone. *J. Appl. Polym. Sci.* **2016**, *133*. [[CrossRef](#)]
5. Wang, B.; Qian, T.; Zhang, Q.H.; Zhan, X.L.; Chen, F.Q. Heat resistance and surface properties of polyester resin modified with fluorosilicone. *Surf. Coat. Technol.* **2016**, *304*, 31–39. [[CrossRef](#)]
6. Yan, Z.L.; Liu, W.Q.; Gao, N.; Wang, H.L.; Su, K. Synthesis and properties of a novel UV-cured fluorinated siloxane graft copolymer for improved surface, dielectric and tribological properties of epoxy acrylate coating. *Appl. Surf. Sci.* **2013**, *284*, 683–691. [[CrossRef](#)]
7. Zhang, M.; Li, J.; Zang, D.L.; Lu, Y.; Gao, Z.X.; Shi, J.Y.; Wang, C.Y. Preparation and characterization of cotton fabric with potential use in UV resistance and oil reclaim. *Carbohydr. Polym.* **2016**, *137*, 264–270. [[CrossRef](#)] [[PubMed](#)]
8. Guo, P.; Zhai, S.R.; Xiao, Z.Y.; An, Q.D. One-step fabrication of highly stable, superhydrophobic composites from controllable and low-cost PMHS/TEOS sols for efficient oil cleanup. *J. Colloid Interface Sci.* **2015**, *446*, 155–162. [[CrossRef](#)]
9. Xue, C.H.; Yin, W.; Jia, S.T.; Ma, J.Z. UV-durable superhydrophobic textiles with UV-shielding properties by coating fibers with ZnO/SiO<sub>2</sub> core/shell particles. *Nanotechnology* **2011**, *22*, 1–8. [[CrossRef](#)]
10. Gonçalves, G.; Marques, P.A.A.P.; Trindade, T.; Neto, C.P.; Gandini, A. Superhydrophobic cellulose nanocomposites. *J. Colloid Interface Sci.* **2008**, *324*, 42–46. [[CrossRef](#)]
11. Daoud, W.A.; Xin, J.H.; Zhang, Y.H.; Mak, C.L. Pulsed laser deposition of superhydrophobic thin Teflon films on cellulosic fibers. *Thin Solid Films* **2006**, *515*, 835–837. [[CrossRef](#)]
12. Zimmermann, J.; Reifler, F.A.; Fortunato, G.; Gerhardt, L.C.; Seeger, S. A simple, one-step approach to durable and robust superhydrophobic textiles. *Adv. Funct. Mater.* **2008**, *18*, 3662–3669. [[CrossRef](#)]
13. Hoefnagels, H.F.; Wu, D.; With, G.D.; Ming, W. Biomimetic superhydrophobic and highly oleophobic cotton textiles. *Langmuir* **2007**, *23*, 13158–13163. [[CrossRef](#)]
14. Zhou, H.; Wang, H.X.; Niu, H.T.; Gestos, A.; Wang, X.G.; Lin, T. Fluoroalkyl silane modified silicone rubber/nanoparticle composite: A super durable, robust superhydrophobic fabric coating. *Adv. Mater.* **2012**, *24*, 2409–2412. [[CrossRef](#)]
15. Li, K.Q.; Zeng, X.R.; Li, H.Q.; Lai, X.J. Fabrication and characterization of stable superhydrophobic fluorinated-polyacrylate/silica hybrid coating. *Appl. Surf. Sci.* **2014**, *298*, 214–220. [[CrossRef](#)]
16. Li, B.C.; Zhang, J.P. Polysiloxane/multiwalled carbon nanotubes nanocomposites and their applications as ultrastable, healable and superhydrophobic coatings. *Carbon* **2015**, *93*, 648–658. [[CrossRef](#)]
17. Hao, L.F.; An, Q.F.; Xu, W. Facile Fabrication of superhydrophobic cotton fabric from stearyl methacrylate modified polysiloxane/silica nanocomposite. *Fiber Polym.* **2012**, *13*, 1145–1153. [[CrossRef](#)]
18. Hao, L.F.; Gao, T.T.; Xu, W.; Wang, X.C.; Yang, S.Q.; Liu, X.G. Preparation of crosslinked polysiloxane/SiO<sub>2</sub> nanocomposite via in-situ condensation and its surface modification on cotton fabrics. *Appl. Surf. Sci.* **2016**, *371*, 281–288. [[CrossRef](#)]
19. Jin, H.; Xu, W. The preparation and properties of fluoroacrylate-modified polysiloxane as a fabric coating agent. *Coatings* **2018**, *8*, 31. [[CrossRef](#)]
20. Xu, W.; An, Q.F.; Hao, L.F.; Zhang, D.; Zhang, M. Synthesis and characterization of self-crosslinking fluorinated polyacrylate soap-free latices with core-shell structure. *Appl. Surf. Sci.* **2013**, *268*, 373–380. [[CrossRef](#)]
21. Xu, W.; An, Q.F.; Hao, L.F.; Huang, L.X. Synthesis, film morphology and performance of cationic fluorinated polyacrylate emulsion with core-shell structure. *J. Appl. Polym. Sci.* **2012**, *125*, 2376–2383. [[CrossRef](#)]
22. Hao, L.F.; An, Q.F.; Xu, W.; Huang, L.X. Synthesis, film morphology and hydrophobicity of novel fluorinated polyacrylate emulsion and solution on silicon wafer. *Colloids Surf. A Physicochem. Eng. Asp.* **2012**, *396*, 83–89. [[CrossRef](#)]
23. Shang, S.-M.; Li, Z.X.; Xing, Y.J.; Xin, J.H.; Tao, X.M. Preparation of durable hydrophobic cellulose fabric from water glass and mixed organosilanes. *Appl. Surf. Sci.* **2010**, *257*, 1495–1499. [[CrossRef](#)]
24. Liu, J.Y.; Huang, W.Q.; Xing, Y.J.; Li, R.; Dai, J.J. Preparation of durable superhydrophobic surface by sol-gel method with water glass and citric acid. *J. Sol-Gel Sci. Technol.* **2011**, *58*, 18–23. [[CrossRef](#)]
25. Cassie, A.B.D.; Baxter, S. Wettability of porous surfaces. *Trans. Faraday Soc.* **1944**, *40*, 546–551. [[CrossRef](#)]

